International Journal of Scientific Research in Engineering and Management (IJSREM)
Volume: 10 Issue: 03 | March - 2026 SJIF Rating: 8.659 ISSN: 2582-3930

Size and Temperature Dependent Memristive Behavior of ZnO Nanoparticles Synthesized via Chemical Bath Deposition

Jyoti prasad roy choudhury[1,2], *Barnalipathak[2]

[1]Assam Don Bosco University, Tepesia, Sonapur, Assam, 782402 ,India

[2]B.H. College ,Howly ,Barpeta, Assam, 781316, India

Corresponding Author: **Jyoti Prasad Roy Choudhury**, Email: jyotirc62@gmail.com,

Abstract

Memristors, theoretically postulated by Leon Chua in 1971 and experimentally realized by Stanley Williams and co-workers at HP Labs in 2008, represent the fourth fundamental passive circuit element and have emerged as promising candidates for next-generation non-volatile memory and neuromorphic systems. In this work, zinc oxide (ZnO) nanoparticles with controlled sizes were synthesized using a polyvinyl pyrrolidone (PVP)-assisted chemical bath deposition (CBD) method. The influence of nanoparticle size and operating temperature on memristive performance was systematically investigated. Structural analysis confirmed the formation of hexagonal wurtzite ZnO with average crystallite sizes of 64.6 nm, 37.3 nm, and 12.1 nm corresponding to 1%, 2%, and 3% PVP concentrations, respectively. Optical band gap values showed slight size dependence, varying from 3.02 to 3.04 eV. Memristive devices fabricated in Ag/ZnO/Ag configuration exhibited clear pinched hysteresis loops. A strong size dependence of the resistance switching ratio (R_OFF/R_ON) was observed, increasing significantly to 22.96 for 12 nm nanoparticles. Temperature-dependent studies (100–300 °C) revealed thermally enhanced switching, with the resistance ratio increasing to 6.7 at 300 °C. The results demonstrate that both nanoparticle size and thermal activation critically govern resistive switching in ZnO-based memristors, highlighting their potential for scalable nanoelectronic and neuromorphic applications.

Keywords: ZnO nanoparticles, memristor, resistive switching, chemical bath deposition, temperature dependence, neuromorphic computing

1. Introduction

The memristor, proposed by Leon Chua, establishes a direct relationship between charge (q) and magnetic flux (Φ), thereby completing the symmetry among the four fundamental circuit variables. Decades later, experimental verification was achieved by Stanley Williams and his team at HP Labs through the demonstration of resistive switching in nanoscale TiO_2 devices. Since then, metal-oxide-based memristors have attracted substantial interest due to their simple structure, low power consumption, scalability, and compatibility with complementary metal–oxide–semiconductor (CMOS) technology.

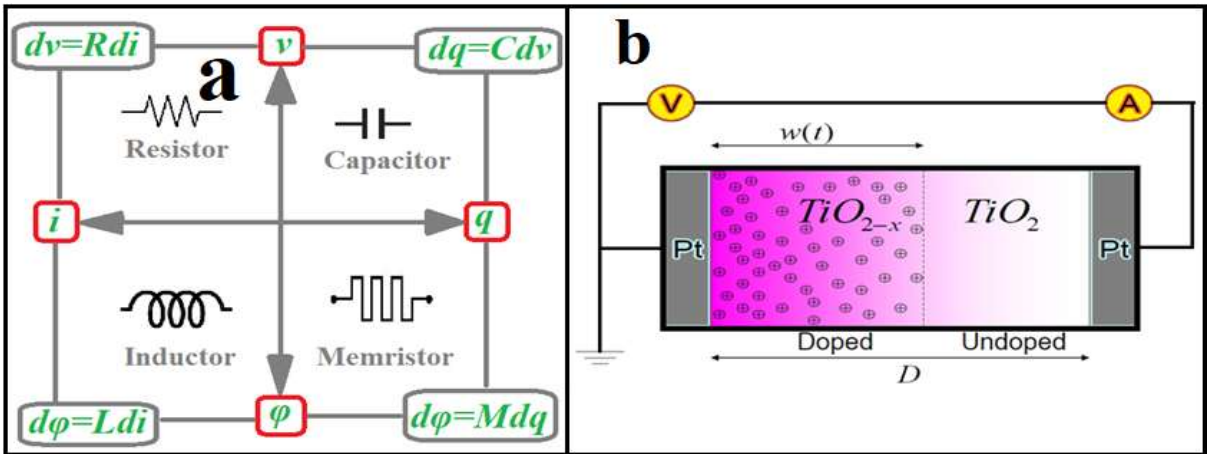

Figure 1: Four fundamental passive electrical components and their relation (a) & HP memristor (b)

Among various oxide materials, zinc oxide (ZnO) is particularly attractive due to its wide direct band gap (~3.3 eV), high exciton binding energy (~60 meV), chemical stability, and defect-rich nature. Oxygen vacancies in ZnO play a decisive role in resistive switching by facilitating conductive filament formation and rupture. Although numerous studies have examined ZnO thin films and nanostructures, systematic investigations correlating nanoparticle size with memristive behavior remain limited.

Additionally, thermal effects significantly influence resistive switching through thermally activated ion migration, Joule heating, and defect redistribution. Understanding temperature-dependent switching mechanisms is therefore essential for device reliability and high-temperature operation.

2. Experimental Methods

2.1 Synthesis of ZnO Nanoparticles

ZnO nanoparticles were synthesized via chemical bath deposition using varying PVP concentrations (1%, 2%, and 3%) as a capping and stabilizing agent. The samples were labeled Z1, Z2, and Z3, respectively. The capping agent regulated nucleation and growth kinetics, enabling particle size control.

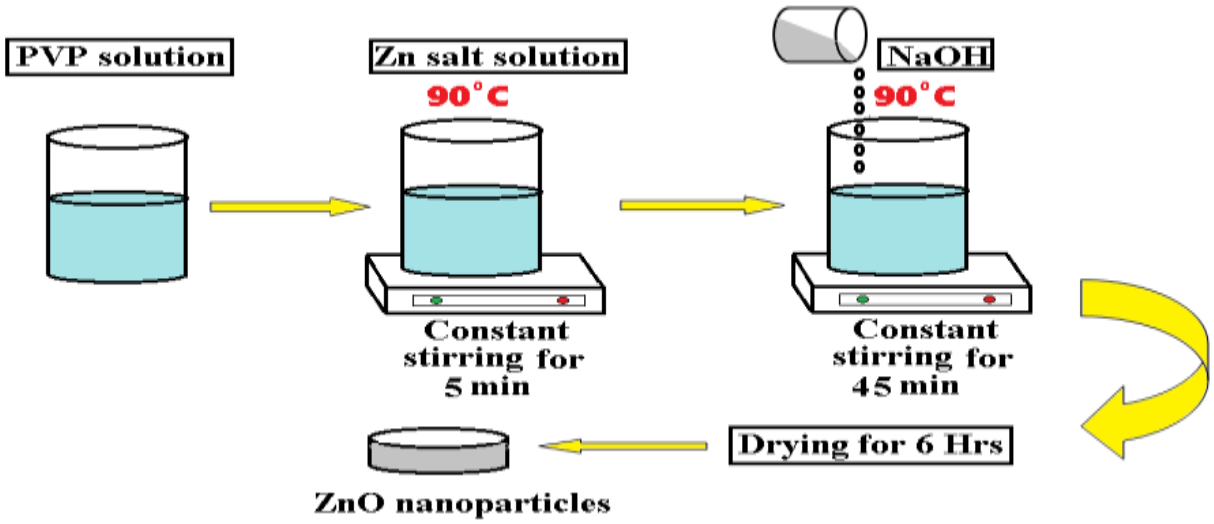

Fig 2. Schematic for preparation of ZnO nanoparticles

2.2 Structural and Morphological Characterization

X-ray diffraction (XRD) confirmed the formation of hexagonal wurtzite ZnO. The crystallite size (D) was estimated using the Debye–Scherrer equation:

$$\frac{1}{d^2} = \frac{4}{3}\left(\frac{h^2 + K^2 + hk}{a^2}\right) + \frac{l^2}{c^2}$$

Where, d = crystalline size, (hkl)= miller indices and a & c = lattice constant.

For hexagonal ZnO nanoparticles the lattice constants are found to be a = 3.2389 Å and c = 5.2010 Å which are close to that of standard JCPDS card no- JCPDS-00-036-1451.

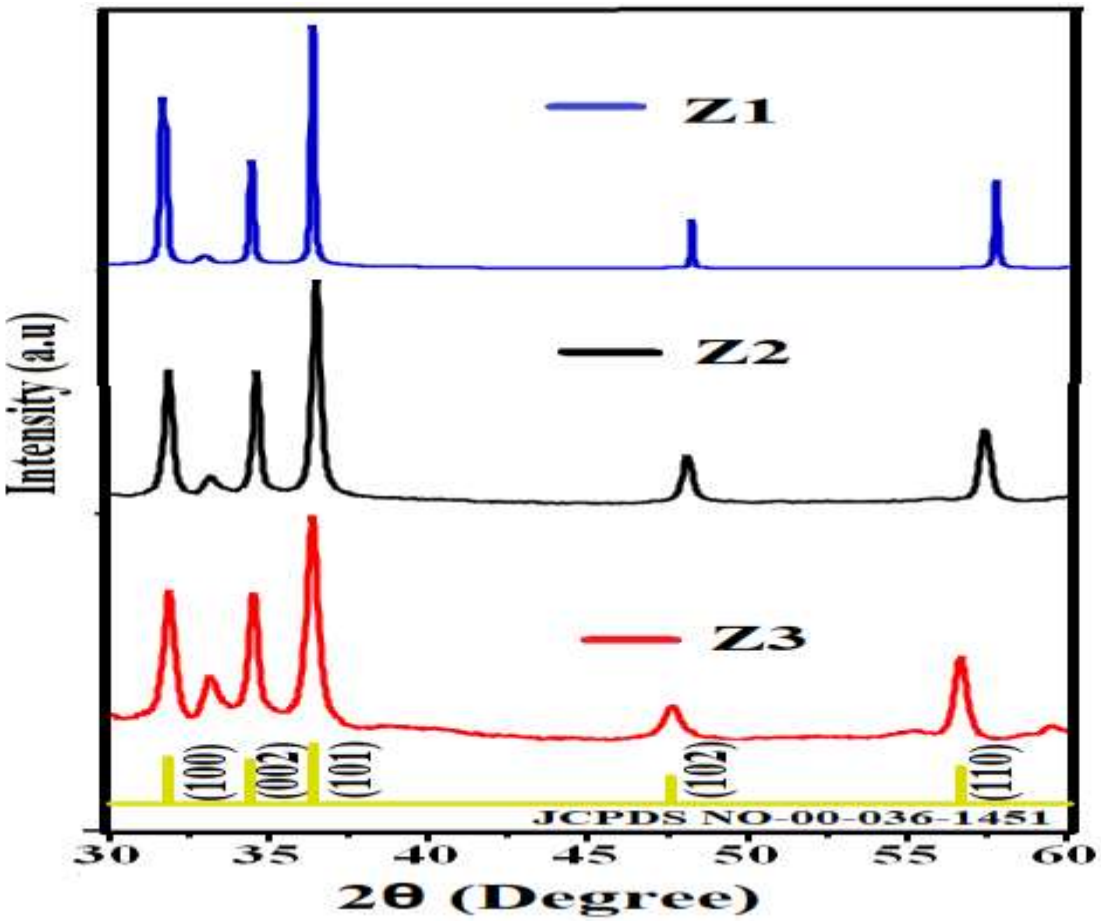

Figure 3: XRD peaks of ZnO nsanoparticles of different sizes.

High-resolution transmission electron microscopy (HRTEM) was employed to verify morphology and particle size distribution.

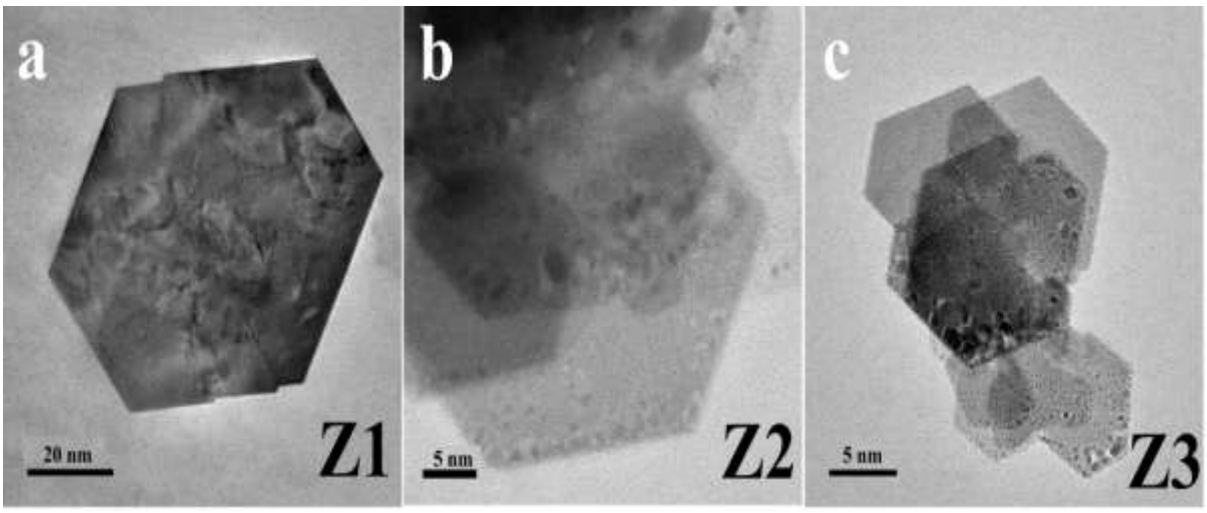

Figure 4: HRTEM image of ZnO nanoparticles of different size.

2.3 Optical Analysis

UV–Visible absorption spectroscopy was conducted to determine the optical band gap using Tauc plots:

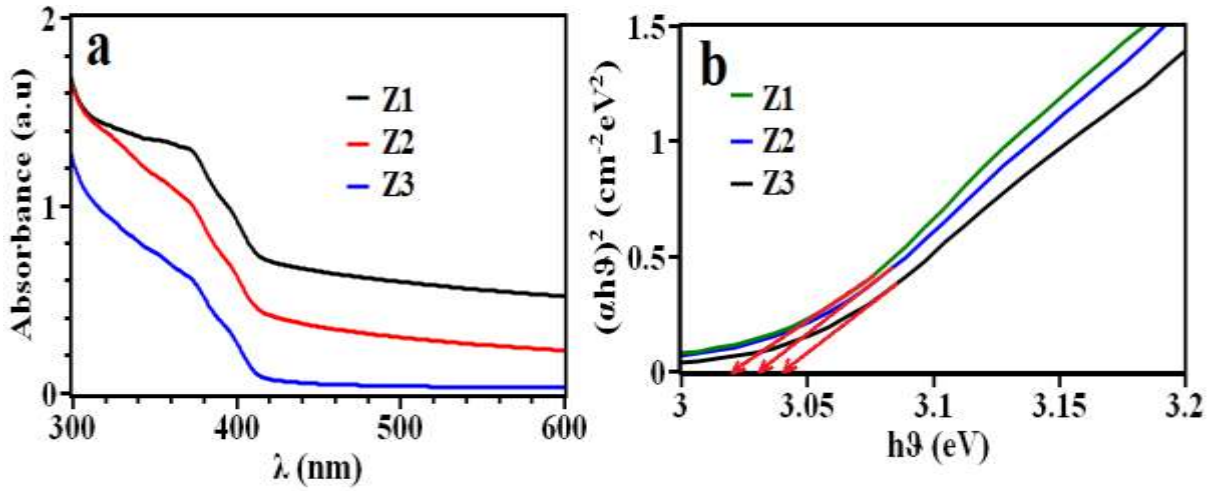

Figure 5. Absorption spectra and their corresponding Taue plot of capping agent varied ZnO nanoparticles.

3. Device Fabrication and Electrical Measurement

Memristive devices were fabricated in a planar Ag/ZnO/Ag configuration with a 1 mm electrode gap. Current–voltage (I–V) characteristics were recorded under DC voltage sweep (–1 V to +1 V). Temperature-dependent measurements were performed at 100 °C, 200 °C, and 300 °C.

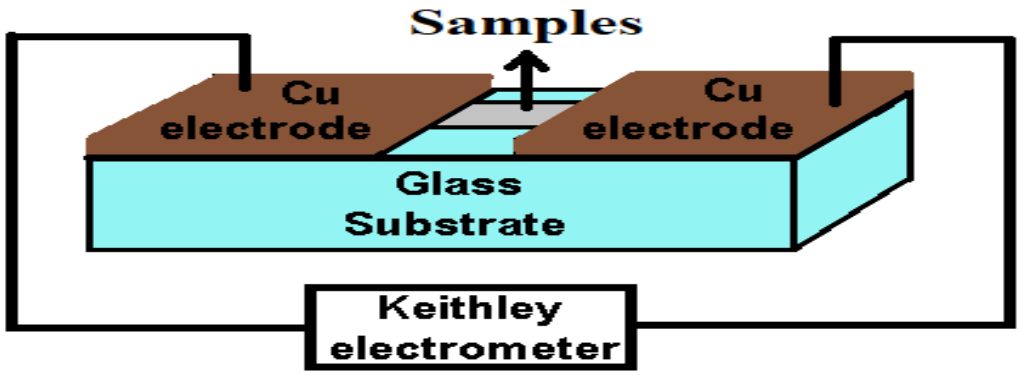

Figure 6: Structure of prepared memristive device

3.1 Structural Properties

XRD patterns exhibited diffraction peaks corresponding to (100), (002), (101), (102), and (110) planes of hexagonal ZnO. The calculated lattice constants (a = 3.2389 Å, c = 5.2010 Å) matched standard values.

Crystallite sizes were determined as:

- Z1: 64.6 nm
- Z2: 37.3 nm

- Z3: 12.1 nm

HRTEM analysis confirmed uniform morphology and strong agreement with XRD-derived sizes.The decrease in particle size with increasing PVP concentration demonstrates effective surface passivation and growth suppression.

3.2 Optical Properties

All samples showed absorption edges near the UV region. The estimated band gaps were:

- Z1: 3.02 eV
- Z2: 3.03 eV
- Z3: 3.04 eV

The slight increase in band gap with decreasing particle size is attributed to quantum confinement and reduced defect density due to improved surface stabilization.

3.3 Size-Dependent Memristive Behavior

All fabricated devices exhibited pinched hysteresis loops characteristic of memristors. The resistance switching ratios were:

Sample	Particle Size	R_{off}/R_{on}
Z1	64.6	1.53
Z2	37.3	1.74
Z3	12.1	22.96

Smaller nanoparticles promote more effective modulation of conductive pathways, leading to improved switching contrast.

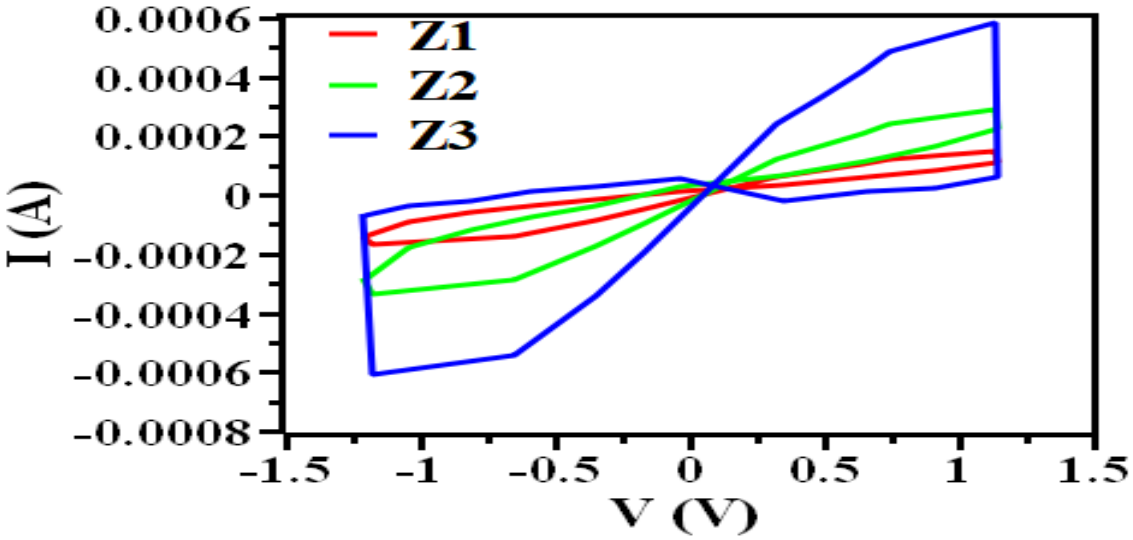

Figure 7: Hysteresis loop of prepared ZnO- based memristor.

3.4 Temperature-Dependent Memristive Behavior

The Z3 sample (13 nm) was selected for thermal analysis. Pinched hysteresis loops were preserved across all temperatures.

Sample	Temperature in degree	R_{off}/R_{on}
Z3	100	1.9
	200	2.0
	300	6.7

The enhanced behavior at elevated temperatures can be attributed to:

1. Thermally activated migration of oxygen vacancies
2. Increased carrier concentration
3. Improved formation of conductive filaments
4. Joule heating–assisted switching

At higher temperatures, increased ionic mobility facilitates vacancy movement, which strengthens resistive modulation and results in a larger hysteresis loop area.

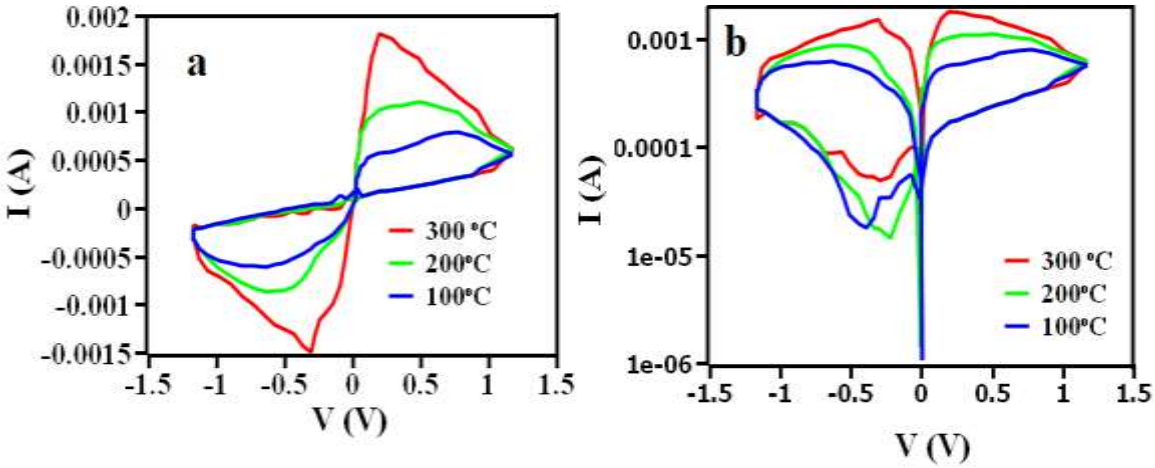

Figure 8: IV characteristic (a) and logarithimic (b) curve showing pinched hysteresis loop of Ag/ZnO/Ag memristive device at different temperatures.

4. Switching Mechanism

Resistive switching in ZnO nanoparticles is governed primarily by a thermo-chemical filamentary mechanism: **SET Process (Low Resistance State):** Electric field drives oxygen vacancies to form conductive filaments. **RESET Process (High Resistance State):** Filaments rupture due to Joule heating and ion redistribution. Temperature accelerates vacancy mobility, thus enhancing filament dynamics and resistance contrast.

5. Conclusion

This investigation clearly shows that both nanoparticle dimension and operating temperature are decisive parameters in determining the memristive performance of ZnO-based devices. By systematically varying the particle size and analyzing electrical characteristics under different thermal conditions, a strong correlation between structural scale and resistive switching behavior has been established.

First, the particle size of ZnO was successfully tuned through a polyvinyl pyrrolidone (PVP)-assisted chemical bath deposition (CBD) process. Increasing the PVP concentration effectively suppressed nanoparticle growth, leading to a controlled reduction in crystallite size. This confirms that the capping agent plays a critical role in regulating nucleation and growth kinetics during synthesis.

Second, optical analysis revealed a slight increase in band gap energy with decreasing particle size. This size-dependent modulation of the optical band gap can be attributed to quantum confinement effects and improved surface passivation, which reduce defect density and alter electronic transitions in nanoscale ZnO.

Most importantly, the electrical measurements demonstrated a dramatic improvement in memristive switching performance as particle size decreased. The resistance switching ratio (R_OFF/R_ON) increased significantly, reaching a value as high as 22.96 for ~12 nm particles. This substantial enhancement is mainly associated with the higher surface-to-volume ratio and increased oxygen vacancy activity in smaller nanoparticles, which facilitate more efficient conductive filament formation and rupture.

Temperature-dependent measurements further revealed that switching behavior is thermally activated. As the operating temperature increased to 300 °C, the R_OFF/R_ON ratio rose to 6.7. Elevated temperatures enhance oxygen vacancy mobility and carrier excitation, strengthening the contrast between high-resistance and low-resistance states. This confirms that thermal energy assists filament dynamics and improves resistive modulation.

The observed switching mechanism is consistent with a filamentary model governed by oxygen vacancy migration. Under an applied electric field, oxygen vacancies drift and accumulate to form conductive paths (SET process), while Joule heating and field redistribution disrupts these filaments during RESET.

Overall, the study demonstrates that careful control of nanoparticle size and thermal conditions can significantly optimize memristive performance. These findings position ZnO nanoparticles as strong candidates for advanced applications such as resistive random-access memory (RRAM), neuromorphic computing hardware, and nanoelectronic systems designed to operate reliably under elevated temperatures.

6. REFERENCES

1. Chua, L. O. (1971). Memristor—The missing circuit element. *IEEE Transactions on Circuit Theory, 18*(5), 507–519. https://doi.org/10.1109/TCT.1971.1083337

2. Strukov, D. B., Snider, G. S., Stewart, D. R., & Williams, R. S. (2008). The missing memristor found. *Nature, 453*, 80–83.

3. Biolek, D., Biolek, Z., Biolkova, V., & Kolka, Z. (2013). Computing areas of pinched hysteresis loops of mem-systems in OrCAD PSPICE. *Applied Computing and Informatics, 278*, 1081–1086.

4. Chua, L. O., & Kang, S. M. (1976). Memristive devices and systems. *Proceedings of the IEEE, 64*(2), 209–223. https://doi.org/10.1109/PROC.1976.10092

5. Laurenti, M., Canavese, G., & Stassi, S. (2016). Memristive devices based on nanomaterials. *RSC Advances, 6*, 76996–77004.

6. Wager, J., Yeh, B., & Hoffman, R. (2014). Electronic materials for memristive devices. *Current Opinion in Solid State and Materials Science, 18*, 53–60.

7. Song, R. Q., Xu, A. W., & Deng, B. (2007). Nanostructured materials for electronic applications. *Advanced Functional Materials, 17*, 296–302.

8. Kurban, M., & Muz, I. (2023). Structural properties of memristive materials. *Structural Chemistry, 34*, 1061–1070.

9. Deylam, M., Alizadeh, E., Sarikhani, M., Hejazy, M., & Firouzamandi, M. (2021). Memristive biomaterials for biomedical applications. *Journal of Materials Science: Materials in Medicine, 32*, 128.

10. Chang, S. P., & Chen, K. J. (2012). Memristor-based nanoelectronic devices. *Journal of Nanomaterials, 2012*, 1–7.

11. Celano, U., Goux, L., Belmonte, A., Detavernier, C., Jurczak, M., & Vandervorst, W. (2014). Three-dimensional observation of conductive filament in nanoscale resistive memory devices. *Nano Letters, 14*, 2401–2406.

12. Sun, K., Zhang, Y., & Meng, J. (2018). Resistive switching behavior in nanoscale devices. *Applied Physics Letters, 112*, 093503.

13. Lin, Y. C., & Chen, J. Y. (2020). Memristor modeling and device applications. *IEEE Transactions on Electron Devices, 67*, 2230–2236.

14. Younis, A., & Chu, D. (2018). Memristive switching in metal oxide nanostructures. *Advanced Electronic Materials, 4*, 1700287. https://doi.org/10.1002/aelm.201700287

15. Kim, S., & Jeong, D. S. (2010). Resistive switching characteristics of memristive devices. *Electrochimica Acta, 55*, 8701–8707.

16. Yoon, J. H., Kwon, D. Y., & Kim, Y. D. (2016). Switching mechanisms in oxide-based memristors. *The Journal of Physical Chemistry C, 120*, 395–403.

17. Chiu, F. C. (2014). A review on conduction mechanisms in dielectric films. *Advances in Materials Science and Engineering, 2014*, 578168.

18. Lee, M. J., Hur, J. H., & Lee, C. (2012). Electrical characteristics of resistive switching memory devices. *Materials Chemistry and Physics, 136*, 455–460.

19. Liu, Q., Long, S., Wang, Q., Zhang, M., Zhang, S., & Huo, Z. (2009). Resistive switching behavior in metal oxide films. *IEEE Electron Device Letters, 30*, 1335–1337.

20. Lien, C. C., & Wu, C. Y. (2011). Conduction mechanisms in resistive switching devices. *Journal of Applied Physics, 110*, 073717.